Catalysis Today 142 (2009) 17–23

Contents lists available at ScienceDirect

Catalysis Today

journal homepage: www.elsevier.com/locate/cattod

Dehydrogenation of propane over Pt-SBA-15 and Pt-Sn-SBA-15: Effect of Sn on the dispersion of Pt and catalytic behavior

M. Santhosh Kumar [a,1,*], De Chen [a], Anders Holmen [a], John C. Walmsley [b,c]

[a] Department of Chemical Engineering, Norwegian University of Science and Technology (NTNU), N-7491 Trondheim, Norway
[b] SINTEF Materials and Chemistry, N-7465 Trondheim, Norway
[c] Department of Physics, Norwegian University of Science and Technology (NTNU), N-7491 Trondheim, Norway

ARTICLE INFO

Article history:
Available online 13 February 2009

Keywords:
Propane dehydrogenation
SBA-15
Platinum
Tin
Dispersion
Particle size effect
TEOM

ABSTRACT

The objective of this work was to gain a better understanding of the influence of Sn on the dispersion of Pt in platinum supported SBA-15 catalysts and thereby on the dehydrogenation of propane (DHP) activity, selectivity to propylene, coking and catalyst stability. To this end, DHP over Pt-SBA-15 and Pt-Sn-SBA-15, prepared by incipient wetness impregnation (IW), was studied at 793 K by means of tapered element oscillating microbalance (TEOM) coupled with on-line gas-chromatography. This allowed us to determine simultaneously the comprehensive information from a single catalysis experiment. The catalysts were characterised by N_2-physisorption, transmission electron microscopy (TEM-EDXS), X-ray diffraction (XRD) and H_2-chemisorption, which revealed that the presence of Sn results in higher Pt dispersion by the formation of Pt–Sn alloy. It is evident from TEOM studies that after 220 min on stream the amount of coke formed is almost three times higher over Pt-Sn-SBA-15-IW than on its counterpart Pt-SBA-15-IW, albeit the former exhibits considerably higher propane conversion, superior selectivity to propylene and stability than the latter. It is demonstrated that propane conversion and coke formation on the catalysts can be correlated with Pt particle size. A modified drain-off effect is proposed to explain the superior selectivity and stability of the bimetallic than the monometallic catalyst.

1. Introduction

For the past several years the demand for propylene has been increasing due to its important role in a myriad of (petro)chemical applications such as in the production of polypropylene, cumene, etc. [1–6]. So far, a major part of the propylene demand has been supplied by conventional crackers such as steam and fluid catalytic (FC) crackers where propylene is produced as a by-product [2,7–9]. Due to the growing demand, the high severity crackers were optimized to increase the production of propylene, however they are governed by the gasoline demand. As a result of this, the rate of propylene recovery from FCC has been increased today to ~80% as compared to 29% in 1980 [8,10]. Nevertheless, these conventional crackers are not keeping up with the propylene demand resulting in a gap between demand and supply. Therefore, *on-purpose* propylene production technologies such as dehydrogenation of propane (DHP) [11,12] and oxidative dehydrogenation of propane (ODHP) [9,13] have been developed. Since then, these technologies have received a great deal of attention due to their potential to make-up the shortfall of propylene supply left by conventional crackers.

Having said that, DHP is a challenging reaction as it is equilibrium limited and highly endothermic thus high temperatures are usually required for reasonable propane conversion [14,15]. The promising catalytic formulations for DHP are based on Pt or Cr catalysts [2,5,6,16,17]. However, major problems associated with these catalytic systems are cracking of long chain hydrocarbons and coke formation. The former reduces the selectivity to propylene and the latter causes deactivation of the catalyst. Thus, the deactivated catalyst must frequently be regenerated without losing dehydrogenation activity, selectivity to propylene and stability, which increases the process complexity and operation costs. Consequently, much research has been devoted to gaining a better knowledge of these dehydrogenation catalytic systems in order to develop them further such that the rate of DHP reaction increases while diminishing undesired side reactions such as cracking and coking, thus prolonging the catalysts life time. Pt-Sn bimetallic catalysts show the above mentioned characteristics to some extent more than the corresponding monometallic Pt catalysts [5,6,18–20]. Despite extensive studies, the role of Sn in a bimetallic catalyst remains elusive and therefore it has been a subject of debate for many years

* Corresponding author. Tel.: +41 44 823 4726; fax: +41 44 823 4041.
E-mail address: santhosh.matam@empa.ch (M. Santhosh Kumar).
[1] Present address: Laboratory for Solid State Chemistry and Catalysis, Eidgenössische Materialprüfungs und Forschungsanstalt (EMPA), CH-8600 Dübendorf, Zürich, Switzerland.

0920-5861/$ – see front matter © 2009 Elsevier B.V. All rights reserved.
doi:10.1016/j.cattod.2009.01.002

[5,6,18–20]. For example, it has been often concluded that Sn reduces coke formation by suppressing cracking, hydrogenolysis and isomerisation, thus increasing catalyst stability [21–25]. In contrast, an increased amount of coke formation was, though seldom, reported on bimetallic Pt-Sn catalyst than on its counterpart monometallic Pt catalyst, albeit the former showing higher selectivity and stability than the latter [26,27]. These contradictory observations were commonly explained by the famous ensemble (geometric) and electronic effects, yet there is no consensus. For example, Cortright et al. have suggested that Sn reduces the size of surface Pt ensembles that inhibits the formation of highly dehydrogenated surface species on large ensembles via undesired side reactions [19,25]. Oppositely, Beloen et al. have shown by kinetic studies that such dehydrogenated surface species can also form on small surface Pt ensembles [20]. Also, our recent studies on DHP over monometallic Pt catalysts are pointing towards the same conclusion [28]. Therefore, in this study we have made an attempt to bring some clarity on the role of Sn.

This work evaluates the influence of Sn on the dispersion of Pt in Pt-SBA-15 and on DHP activity, selectivity to propylene, the degree of coking and catalyst stability. To this end, a tapered element oscillating microbalance (TEOM) coupled with an on-line gas-chromatography (GC) was used. This allows us to derive comprehensive information from a single catalysis experiment and for the first time we will provide direct evidence for the formation of higher amount of coke on bimetallic Pt-Sn catalyst than that on monometallic Pt catalyst.

2. Experimental

2.1. Preparation of catalysts

The parent siliceous SBA-15 was prepared in our laboratory according to the procedure reported in the literature [29,30]. Briefly, a gel prepared from pluronic P123 (EO_{20} PO_{70} EO_{20}, BASF), the template, 2 M HCl and tetraethylorthosilicate (TEOS, Alfa Aesar, 99%), silicon source, was stirred at 313 K for 24 h. The gel was then transferred into a teflon bottle and aged in an oven at 373 K for 48 h. The resulting white solid was filtered, washed thoroughly with double deionised water and dried at room temperature for 24 h. The final product was then calcined in flowing air at 823 K for 6 h to remove the template and thereby to produce mesoporous SBA-15.

Monometallic Pt and bimetallic Pt-Sn catalysts were prepared by incipient wetness impregnation. Impregnation solutions were prepared by dissolving appropriate amounts of $Pt(NH_3)_4(NO_3)_2$ (Johnson-Matthey/Aesar) and $SnCl_2{\cdot}2H_2O$ (Merck, 98–100%) in double deionised water. The resulting solution was added dropwise to the pristine siliceous SBA-15 support, which had been pretreated in an oven at 373 K for 16 h. Bimetallic Pt-Sn catalyst was prepared by consecutive impregnation of Sn followed by Pt. After impregnation of each metal, the samples (mono and bimetallic catalysts) were dried at 373 K for 16 h and subsequently calcined in flowing air at 673 K for 4 h with a heating rate of 5 K min^{-1}. The composition and textural properties of the support SBA-15 and the catalysts are presented in Table 1.

2.2. Characterisation techniques

Nitrogen adsorption and desorption isotherms at 77 K were obtained on a Micromeritics TriStar 3000 instrument. Prior to the experiments, the samples were evacuated at 473 K for 12 h. The micropore volumes (V_{micro}) were determined by the *t*-plot method according to Harkins and Jura's expression [31]. The total surface area of the samples was determined by the Brunauer–Emmett–Teller (BET) method. The pore size distributions were obtained from the desorption branch of the isotherm using the Broekhoff–de Boer (BdB) model [32].

Table 1
Chemical composition and textural properties of the catalysts.

Catalyst	Pt[a] (wt.%)	Sn[a] (wt.%)	V_{micro}[b] ($cm^3\ g^{-1}$)	V_{total} ($cm^3\ g^{-1}$)	S_{BET}[c] ($m^2\ g^{-1}$)	Pore size[d] (nm)
SBA-15	–	–	0.066	1.2	850	6.6
Pt-SBA-15	1.3	–	0.031	0.86	540	6.7
Pt-Sn-SBA-15	1.3	1.2	0.035	0.83	504	6.7

[a] Nominal loading.
[b] *t*-Plot method.
[c] BET method.
[d] BdB model applied to the desorption branch of the isotherms.

Transmission Electron Microscopy (TEM) experiments were performed using a JEOL 2010F microscope operated at 200 kV. The catalysts were dispersed in double deionised water and dropped on carbon-film coated copper grids and dried in air. Approximately a hundred Pt particles were measured for determination of an average particle size (Table 2).

The powder X-ray diffraction (XRD) patterns of the samples were collected by a Siemens D-5005 instrument using Cu Kα radiation (λ = 1.542 Å). Low-angle XRD patterns were collected from 2θ of 0.5° to 5° to study the structural ordering of SBA-15. High-angle XRD data were collected in the 2θ range of 20–90° using a step size of 0.02° and a step time of 19 s. The average Pt particle size was calculated from the full width at half-maximum (FWHM) of Pt(1 1 1) reflection using the Scherrer equation (Table 2).

The Pt dispersion was determined by H_2-chemisorption measurements using Micromeritics ASAP2010 Chemi instrument. Reversible isotherms were measured with an interim 30 min evacuation between isotherms. Samples were reduced in a flow of H_2 at 673 K for 4 h followed by evacuation at 473 K for 30 min and cooled to room temperature. At this temperature, samples were once again evacuated for 15 min and H_2-chemisorption experiments were performed. The amount of adsorbed hydrogen was determined by extrapolating the isotherms to zero pressure. The dispersion was determined based on the irreversible uptakes and using an adsorption stoichiometry of unity of hydrogen and platinum. Hemispherical particle sizes were determined from d (nm) = 1.13/D, where D is the metallic dispersion (Table 2).

The catalysts activity, selectivity, coking and stability were simultaneously studied by tapered element oscillating microbalance (TEOM) which is coupled to an on-line GC. To this end, the TEOM (Series 1500 PMA, Rupprecht and Patashnick Co.) with a high resolution microbalance that generates real-time measurements of mass changes during gas–solid reactions [33] was employed. The TEOM reactor connected to a gas dosing system containing mass flow controllers (Bronkhorst) was placed within a heatable stainless steel pressure vessel. Two gas streams were fed to the reactor: (i) reaction mixture (main gas) that passes through the catalyst bed and (ii) the inert gas (purge gas) sweeps the

Table 2
Average Pt particle size of the catalysts and their initial turnover frequencies (TOF) in the DHP reaction.

Catalyst	Particle size (nm)			TOF S^{-1}[c]
	TEM	XRD[a]	H_2-chemisorption[b]	
Pt-SBA-15	21	21	37	0.20
Pt-Sn-SBA-15	10	10	25	0.157

[a] Based on the Scherrer equation.
[b] Determined by d (nm) = 1.13/D (D = dispersion).
[c] TOF calculated, based on H_2-chemisorption data, for initial C_3H_8 conversion (Fig. 4a).

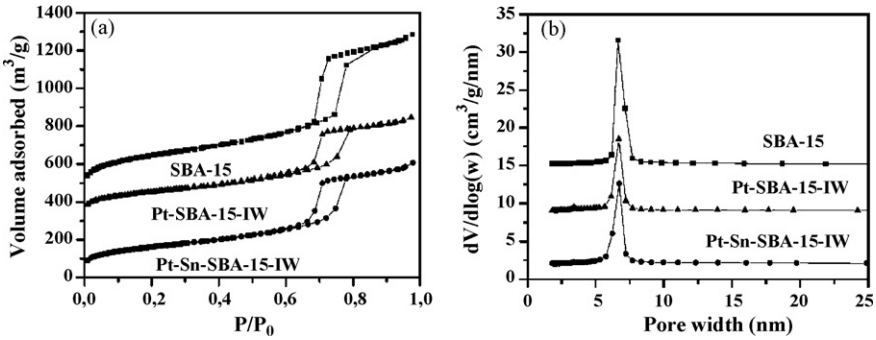

Fig. 1. N_2 adsorption–desorption isotherms of the catalysts (a) and the corresponding pore size distribution as obtained from the desorption branch (b).

volume outside the catalyst bed. The combined flow of both main and purge gas streams were connected to an outlet that serves as a transfer line to a GC. Gas flows, temperatures, TEOM operation and data collection were controlled using Lab-View software [17,28].

The TEOM reactor was loaded with 30 mg of catalyst (sieve fraction ~250 mm), firmly packed between two plugs of quartz wool and retained there by a ventilated metal cap. Prior to the experiments the catalysts were pre-treated in flowing H_2 (20 ml min^{-1}) at the reaction temperature (793 K) for 4 h, by when a stable baseline was reached. Hence, H_2 was replaced by the DHP reaction mixture of C_3H_8 (8 vol.%) and H_2 (13 vol.%) in He at a total flow of 150 ml min^{-1}. The reaction mixture was preheated at 723 K in the preheating zone before entering on to the catalyst bed. A purge gas (He) flow of 200 ml min^{-1} was used. The space velocity (SV) was calculated as $g_{propane}\ g_{cat}^{-1}\ h^{-1}$ and was 47 h^{-1}. The coke content was determined from the mass change measured during reaction. The product gases were analysed by an on-line GC (HP 5890) equipped with a FID, using GS-Q column (30 m length and 0.543 mm i.d., allowing the separation of hydrocarbons up to C_3) and controlled by HP ChemStation software. The product selectivities were calculated on the basis of carbon. The reaction rates (r), mole propane $g_{Cat}^{-1}\ h^{-1}$, were calculated by assuming differential conditions in the catalyst bed. Initial reaction rates (r_o) were determined by plotting the reaction rate (r) against the coke content on the catalyst and thereby extrapolating to zero coke content according to Eq. (1):

$$r = r_o \exp(-\alpha C) \quad (1)$$

where C is the coke content in wt.% and α is a deactivation constant.

3. Results and discussion

3.1. Characterisation of catalysts

The chemical composition and textural properties of the samples are compared in Table 1. The N_2 adsorption–desorption isotherms of the pristine and metal supported SBA-15 are shown in Fig. 1a. The isotherms of the samples show the characteristic behavior of ordered mesoporous materials exhibiting an irreversible type IV isotherm with a well-defined hysteresis loop of type H1 at $p/p0 > 0.66$ [17,30]. This clearly indicates that the mesoporous structure is not disrupted after metal loading. The pore diameter distribution of the samples was determined by the BdB model applied to the desorption branch of the isotherms. It predicts a pore diameter of 6–7 nm in the pristine SBA-15 and is more or less the same in the catalysts (Fig. 1b). The total BET surface area of the pristine sample was determined to be 850 $m^2\ g^{-1}$. However, as expected, the total BET surface area of the catalysts decreased after metal loading as compared to the pristine SBA-15 indicating that some of the metal particles may be located inside the pores (Table 1).

Fig. 2 shows TEM images of the catalysts and it can be clearly seen that Pt particles are larger in Pt-SBA-15-IW than that in Pt-Sn-SBA-15-IW. In the former, the particles are not well distributed and the average size is around 21 nm. In contrast, Pt-Sn-SBA-15-IW contains much smaller particles which are homogeneously distributed. The particle size distribution is narrow and the average bimetallic particle size was determined to be 10 nm. Energy dispersive X-ray spectroscopy (EDXS) points to the formation of Pt–Sn alloy particles. This is in good agreement with

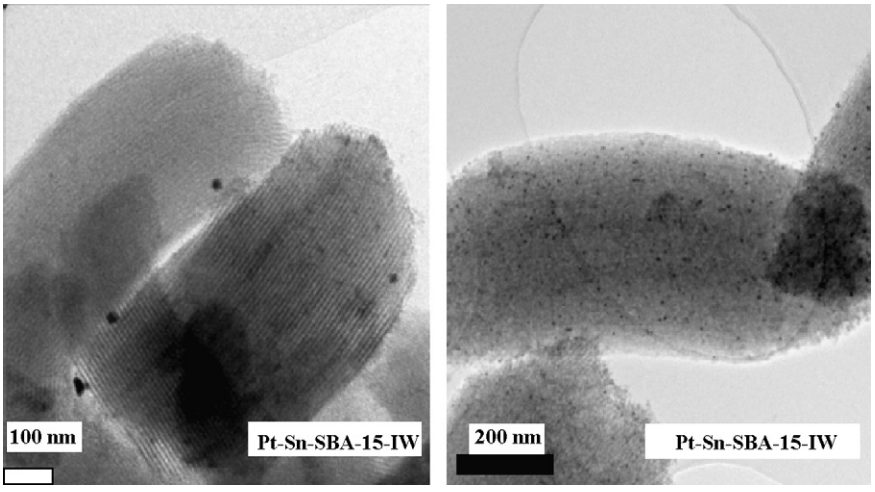

Fig. 2. Transmission electron microscope images of the catalysts.

previous studies which suggest that Sn can easily form an alloy with Pt when it is supported on SiO_2 rather than on Al_2O_3 [6,19,34]. This is due to the fact that Sn can be readily reduced on SiO_2 but not on Al_2O_3 [6,35]. On the latter, it was found that Sn is in oxidized state, often in +2, even after reductive treatment with H_2 [6,36]. TEM micrographs clearly show that Sn, indeed, results in higher Pt dispersion as concluded previously, for example in [5,6,19,35,36]. Additionally, well ordered uniform mesoporous channels of SBA-15 can be directly visualized from these TEM images.

Low-angle XRD patterns (not shown) of the pristine SBA-15 show three characteristic mesostructure reflections at 2θ of 0.98°, 1.62° and 1.82°. These reflections are due to (1 0 0), (1 1 0) and (2 0 0) of the two dimensional *p6mm* hexagonal mesostructure, respectively [37]. Also, Pt-SBA-15-IW and Pt-Sn-SBA-15-IW show these XRD reflections indicating that the hexagonal mesostructure is intact even after metal loading followed by subsequent drying and calcination, in good agreement with N_2-physisorption data and TEM observations.

High-angle XRD patterns of the catalyst are compared in Fig. 3. As expected, Pt-SBA-15-IW shows four characteristic XRD reflections of the large Pt particles at 2θ of 39.8°, 46.2°, 67.4° and 81.1°. These XRD reflections are often assigned to (1 1 1), (2 0 0), (2 2 0) and (3 1 1) inter planar spacings of the cubic platinum metal structure, respectively [28,37]. The average Pt particle size as determined from the FWHM of Pt (1 1 1) peak is 21 nm, which is in good agreement with the TEM observations. However, the observed XRD reflections in Pt-SBA-15-IW are weak/broad in Pt-Sn-SBA-15-IW indicating that the latter contains much smaller particles as compared to the former. The average particle size was determined to be 10 nm which is also in line with the TEM results.

In general, the average Pt particle sizes as determined by H_2-chemisorption is also in agreement with TEM and XRD results as shown in Table 2. However, in particular, the average Pt particle size as determined by H_2-chemisorption is larger than that by TEM and XRD. Such a discrepancy in the particle size determined by H_2-chemisorption and TEM and/or XRD is frequently discussed [5,28,37,38]. A plausible reason could be strong interactions between metal and support or metal and metal (in the case of bimetallic catalyst) [5,6,24,28]. Nevertheless, the dispersion data still show a trend that is in line with the TEM and XRD observations (Table 2).

In summary, N_2-physisorption data, TEM micrographs and low-angle XRD patterns of the pristine SBA-15 show well ordered hexagonal mesostructure, which is virtually intact even after metal loading onto the support and followed by subsequent pre-treatments (drying and calcination). The average Pt particle size in Pt-SBA-15-IW and Pt-Sn-SBA-15-IW as determined by TEM, XRD and H_2-chemisorption shows that Sn results in higher Pt dispersion by alloy formation with Pt, as evidenced by EDXS. Consequently, Pt-Sn-SBA-15-IW contains much smaller bimetallic Pt-Sn particles with an average size of ~10 nm while, Pt-SBA-15-IW contains larger monometallic Pt particles with an average size of ~21 nm. Further, considering the pore diameter of the support SBA-15, as evidenced by N_2-physisorption data (Table 1), and metal particle sizes, as determined by TEM, XRD and H_2-chemisorption (Table 2), it can be suggested that the majority of particles might be located outside the pores.

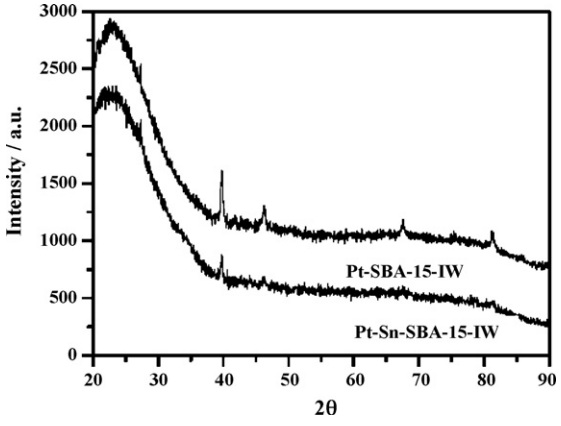

Fig. 3. XRD patterns of the catalysts.

3.2. Dehydrogenation of propane

Fig. 4a shows C_3H_8 conversion and coke formation over Pt-SBA-15-IW and Pt-Sn-SBA-15-IW at 793 K. Initial C_3H_8 conversion values correspond to the analysis of reaction products after 5 min on stream. Bimetallic Pt-Sn-SBA-15-IW that contains smaller particles shows considerably higher C_3H_8 conversion during the whole time on stream studied here compared to Pt-SBA-15-IW which contains larger particles. However, the latter catalyst shows slightly higher specific activity with respect to the surface Pt sites (TOF) than the former (Table 2). The most interesting observation is the formation of coke during the DHP reaction. The amount of coke deposits after 220 min on stream was measured to be almost three times higher on Pt-Sn-SBA-15-IW than that on Pt-SBA-15-IW (Fig. 4a). Despite this, propane conversion (~16%) and selectivity to propylene (~99%) are virtually unchanged over Pt-Sn-SBA-15-IW. Differently, propane conversion gradually decreases from 13 to 11% and selectivity to propylene varies between 84 and 77% over Pt-SBA-15-IW. In addition to propylene being the main product, methane, ethane and ethylene are also formed as by-products over both the catalysts. Among these by-products, methane is the most dominating followed by ethane and ethylene. However, the formation of all these by-products is almost negligible on Pt-Sn-SBA-15-IW as compared on Pt-SBA-15-IW. Hence for the sake of clarity, only selectivity to methane, besides propylene selectivity, is shown for both catalysts (Fig. 4b).

These results provide a sound evidence for the formation of significantly increased amount of coke over bimetallic Pt-Sn catalyst as compared to over monometallic Pt catalyst without influencing the activity and selectivity. This is further supported by

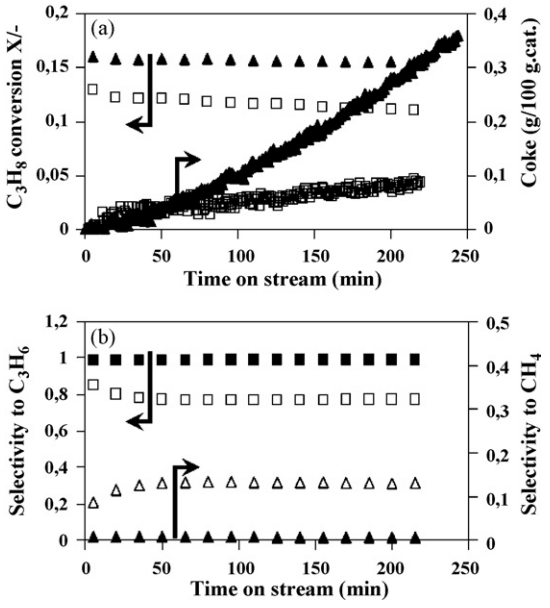

Fig. 4. Pt-SBA-15-IW (open symbols) and Pt-Sn-SBA-15-IW (filled symbols): (a) C_3H_8 conversion and coke formation during DHP and (b) selectivity to C_3H_6 (□, ■) and CH_4 (△, ▲).

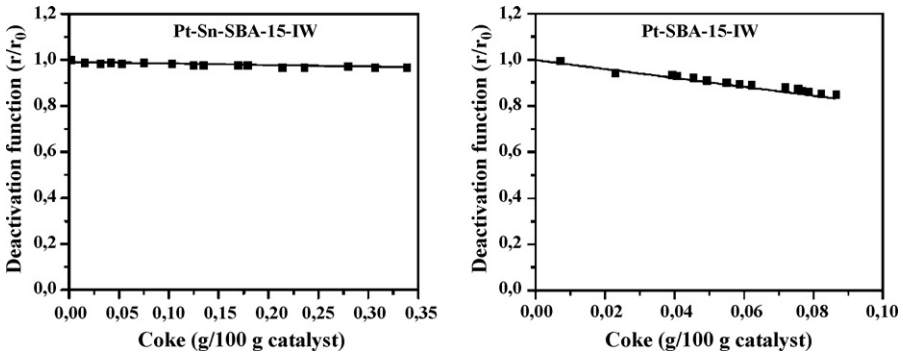

Fig. 5. Catalyst stability: deactivation functions (r/r_o) *vs* coke content.

deactivation functions which are used for studying the catalyst stability, as shown in Fig. 5. Deactivation functions are derived from the same catalytic data that is shown in Fig. 4a. The resulting deactivation functions (r/r_o) are plotted against the amount of coke formation during the reaction. It can be clearly seen from Fig. 5 that despite high amount of coke formation on Pt-Sn-SBA-15-IW, the relative loss in reaction rate is much lower while, it is more significant on Pt-SBA-15-IW even though the amount of coke deposition is much lower. The relative loss in reaction rate is only 4% for Pt-Sn-SBA-15-IW whereas it is almost 20% for Pt-SBA-15-IW. Furthermore, it is clearly visible from the propane conversion profiles itself (Fig. 4a), in which propane conversion is virtually not affected over bimetallic catalyst while it is gradually decreasing over monometallic catalyst.

From the above results it is evident that Pt-Sn-SBA-15-IW shows higher activity and much superior selectivity to propylene than that by Pt-SBA-15-IW, in good agreement with numerous previous studies [5,6,18–25]. However, it is also evident from this study that the amount of coke formed over Pt-Sn-SBA-15-IW is much higher than that on Pt-SBA-15-IW. This observation is in contradiction with most of the previous reports which conclude that Sn reduces the formation of coke [21–25]. Nonetheless, a very few previous studies did report higher amount of coke formation over bimetallic Pt-Sn catalysts (for example on Pt-Sn-Al_2O_3) than that on monometallic Pt catalysts based on temperature programmed oxidation (TPO) studies, though the difference in the amount of coke formed over both the catalysts was marginal [26,27]. In the previous studies, the discrepancy in the amount of coke formation on mono and bimetallic catalysts might have been due to different experiments and/or experimental setups used for determination of catalysts activity and for the amount of coke formed on the catalysts. Usually, catalysis was performed in a plug-flow fixed bed reactor and subsequently the amount of coke (from coked catalysts) was determined by TPO in which effluent gas analysis is crucial. Differently, in the present study we could overcome such biased results by using a novel TEOM reactor that allowed us to determine simultaneously activity, selectivity, the amount of coke formation and thus the catalyst stability. This demonstrates the ability of TEOM/GC system for deriving the comprehensive data from a single catalysis experiment [28].

So far, the behavior of monometallic Pt and bimetallic Pt-Sn catalysts was commonly explained by particle ensemble and electronic effects [19–25]. The famous ensemble effect states that in a bimetallic Pt-Sn particle the long range order of contiguous Pt atoms is interrupted by Sn atoms. This implies that adjacent Pt atoms are separated by Sn atoms that result in an increased distance between the adjacent Pt atoms. Hence, it was concluded that due to increased distance between adjacent Pt atoms the interactions between hydrocarbon and multiple adjacent Pt sites are avoided. This in turn leads to less C–C and C–H bond rupture. For electronic effect it was suggested that Sn significantly changes the electronic properties of Pt atoms in a bimetallic Pt-Sn particle such that the strength of the interactions between Pt and hydrocarbons is reduced [19–25]. Based on these two hypotheses, the higher selectivity to desired dehydrogenated product and lower amount of coke formation was claimed for bimetallic Pt-Sn catalysts than that for monometallic Pt catalysts, in which Pt atoms are contiguous with inherent electronic properties [19–25]. In contrast, our results cannot be completely explained by these two hypotheses, in particular by particle ensemble effect. This is due to the fact that according to particle ensemble effect the Pt-SBA-15-IW that contains larger monometallic Pt particles (~21 nm), in which long range order of contiguous Pt atoms exist, would show higher activity and larger amount of coke formation than that by Pt-Sn-SBA-15-IW that contains much smaller Pt-Sn particles (~10 nm), in which adjacent Pt atoms are interrupted by Sn atoms (Table 2). However, our observations on the activity and on the coke formation are in fact opposite (Fig. 4a) ruling out the particle ensemble effect. Differently, our results can be explained by a particle size effect and by a combination of electronic and drain-off effects as discussed below.

Recently we have shown that Pt particle size does not only influence the catalyst activity but also plays a crucial role in determining selectivity and catalyst stability [28]. Smaller Pt particles are more active for propane conversion and coke formation than larger Pt particles however, the former are less selective and stable than the latter. These observations were attributed to different surface site heterogeneity (surface roughness) of Pt particles. To extrapolate, the surface site heterogeneity (i.e., the fraction of highly coordinatively unsaturated surface Pt atoms) increases with decreasing particle size. This is due to the fact that in smaller particles the surface is mostly terminated by steps, edges, etc., where Pt atoms are highly coordinatively unsaturated. Differently, in larger Pt particles the surface is mainly terminated by terraces and planes where Pt atoms are relatively coordinatively saturated [28,37,39]. The highly coordinatively unsaturated surface Pt sites, which are highly active, especially for C–C bond rupture, in monometallic Pt catalyst cause complete cracking of hydrocarbons that leads to coke deposits and thus catalyst deactivation [28,37,40]. Furthermore, it has recently been shown by in situ FT-IR of adsorbed CO studies that Sn (in Pt-Sn supported on hydrotalcite catalysts) is mainly deposited at highly coordinatively unsaturated surface Pt sites leading to modified electronic properties of the Pt sites [41]. Therefore, it was concluded that by preferential covering of these high energetic Pt sites by Sn reduces the catalytic cracking activity and hence increases the selectivity and catalyst stability. However, the authors have not discussed the influence of Sn on the formation of coke [41]. Additionally, it is also evident from the literature that the effect of Sn on the induced electronic properties of Pt depends on the Pt particle sizes, it being significant for smaller particles than larger ones [42].

Based on the above discussion it can be suggested that the catalytic performance of monometallic Pt-SBA-15-IW and bimetallic Pt-Sn-SBA-15-IW can be due to the difference in particle size as evidenced by TEM, XRD and H_2-chemisorption (Table 2). As a result of different particle sizes in the catalysts, the surface roughness of the particles in the catalysts is, expected to be, different [28]. Consequently, Pt-Sn-SBA-15-IW shows higher propane conversion and higher amount of coke formation compared to Pt-SBA-15-IW which contains larger Pt particles. Nonetheless, the possibility of the promoting effect of Sn on the formation of coke cannot be completely ruled out. This can only be answered by studying the catalytic performances of mono and bimetallic catalysts with similar particle sizes, further studies to this end are in progress. However, despite higher amount of coke formation on Pt-Sn-SBA-15-IW, it still exhibits much higher selectivity to propylene and catalyst stability than its counter part Pt-SBA-15-IW, which cannot be explained by the effect of the size of Pt particles. But these observations can be explained by a combination of electronic and drain-off effects rather than by the electronic effect alone.

As such the electronic effect has been extensively discussed [19–25,41,42]. Differently, the drain-off effect, that has been widely ignored, was first proposed by Lieske et al. and it is discussed in the context of particle ensemble effect [43]. It suggests that coke precursors such as olefinic species adsorb less strongly on the Pt-Sn bimetallic catalyst due to an ensemble effect of Sn. Therefore, coke precursors are mobile and easily migrate to the support where they finally deposit as coke. In this study, we propose the modified drain-off effect which is based on a combination of the electronic and drain-off effects. In Pt-Sn-SBA-15, Sn might have preferentially located at highly coordinatively unsaturated surface Pt sites of bimetallic alloy Pt-Sn particles, as reported previously [41]. Consequently, the degree of unsaturation in the coordination sphere of Pt sites decreases and interactions between Pt and Sn increase which modifies electronic properties and, thus, catalytic properties of Pt sites. Interactions between Pt and Sn weaken the chemisorption properties of Pt sites, leading to weaker interactions between the Pt sites and hydrocarbons, which is also evident from the literature. The addition of Sn to Pt catalyst reduces the strength of interaction of H_2, CO and C_2H_2 with Pt sites [19,20,44]. Accordingly, we assume weaker interactions between Pt sites and propane, this in turn has two implications: (i) selective C–H bond activation is favoured over C–C and C–H bond rupture, leading to high selectivity to propylene and (ii) coke precursors such as (partly)dehydrogenated hydrocarbons can easily move on the surface of Pt-Sn particles and thus they migrate from active sites to the support before being completely converted into coke [43]. In other words, Sn acts as a scavenger to keep Pt sites *clean* from coke by draining-off the coke precursors from the vicinity of active sites to the support, which acts as a reservoir for coke deposits. Therefore, bimetallic catalyst Pt-Sn-SBA-15-IW shows higher selectivity to propylene and much better stability than its counter monometallic catalyst Pt-SBA-15-IW, albeit high amount of coke formation.

Finally, bearing in mind that Pt-Sn-SBA-15-IW contains smaller Pt particles (i.e., higher Pt dispersion) than Pt-SBA-15-IW, the observed lower initial specific activity (TOF) of Pt in the former than that in the latter might be due to either induced electronic effect or deposition of Sn on some of the surface Pt sites, as discussed above and also suggested in [6,24,42,45]. Such a low initial specific activity (in DHP) of Pt in Pt-Sn-SiO_2 with that in Pt-SiO_2 was also observed previously and attributed to the formation of alloy of Pt–Sn and hence the modified electronic configuration of Pt sites [6,45].

4. Conclusions

Pt-SBA-15 and Pt-Sn-SBA-15, prepared by incipient wetness impregnation (IW), were characterised by N_2-physisorption, TEM, XRD and H_2-chemisorption to investigate the influence of Sn on the dispersion of Pt, and thereby on the activity, selectivity, coking and catalyst stability. Dehydrogenation of propane over these catalysts was studied at 793 K by means of TEOM coupled with an on-line GC. Based on these results, the following main conclusions can be drawn:

- Sn results in higher Pt dispersion by alloy formation in Pt-Sn-SBA-15-IW. This leads to the formation of smaller Pt particles in Pt-Sn-SBA-15-IW than in Pt-SBA-15-IW as evidenced by TEM, XRD and H_2-chemisorption.
- The nature and activity properties of surface Pt sites in the catalysts are different due to differences in surface roughness (i.e., surface site heterogeneity) of the particles. Additionally, catalytic properties of Pt sites are influenced by modification of electronic properties of the same sites by Sn in bimetallic Pt–Sn alloy particles (Pt-Sn-SBA-15-IW).
- Higher propane conversion and higher amount of coke formation on smaller Pt particles (Pt-Sn-SBA-15-IW) than on the larger (Pt-SBA-15-IW) are due to higher surface roughness of the former than that of the latter. However, the promoting effect of Sn on coke formation is not completely ruled out.
- Pt-Sn-SBA-15-IW exhibits higher selectivity to propylene and superior catalyst stability than that of Pt-SBA-15-IW due to weaker adsorption affinity of hydrocarbons on the surface Pt sites in Pt-Sn bimetallic particles. Thus, it creates a draining-off effect that keeps active sites *clean* from coking.

Acknowledgements

The Norwegian Research Council (NFR) is gratefully acknowledged for financial support. We thank Assoc. Prof. Gisle Øye for allowing us to use his lab for the preparation of the SBA-15 support.

References

[1] D. Sanfilippo, Cattech 41 (2000) 56.
[2] D. Akporiaye, S.F. Jensen, U. Olsbye, F. Rohr, E. Rytter, M. Ronnekleiv, A.I. Spjelkavik, Ind. Eng. Chem. Res. 40 (2001) 4741.
[3] E. Rytter, H. Bolt, Proc. CatCon, Houston, USA, 2000.
[4] Anon., Euro. Chem. News 67 (1997) 28.
[5] L. Bendnarova, C.E. Lyman, E. Rytter, A. Holmen, J. Catal. 211 (2002) 335.
[6] O.A. Barias, A. Holmen, E.A. Blekkan, J. Catal. 158 (1996) 1.
[7] P. Eisele, R. Killpack, Ullmann's Encyclopedia of Industrial Chemistry, 6th ed., Villey-CCH, Weinheim, 1998.
[8] F. Cavani, N. Ballarini, A. Cericola, Catal. Today 127 (2007) 113.
[9] C. Demay, Petr. Tech. 429 (2000) 75.
[10] C. Marcilly, J. Catal. 216 (2003) 47.
[11] G. Egloff, C.L. Thomas, C.B. Linn, Ind. Eng. Chem. 28 (1936) 1283.
[12] A.H. Tullo, Chem. Eng. News 81 (2003) 15.
[13] F. Cavani, F. Trifire, in: J.J. Spivey (Ed.), Specialist Periodical Reports: Catalysis, vol. 11, Royal society of Chemistry, London, 1994, p. 246.
[14] G.M. Panchenkov, A.S. Kazanskaya, A.D. Pershin, Neftekhimiya 7 (6) (1967) 858.
[15] F. Cavani, F. Trifire, Chim. Ind. 76 (1994) 708.
[16] F.E. Frey, H.F. Huppke, Ind. Eng. Chem. 25 (1933) 54.
[17] M. Santhosh Kumar, N. Hammer, M. Rønning, A. Holmen, D. Chen, J.C. Walmsley, G. Øye, J. Catal 261 (2009) 116.
[18] T. Waku, J.A. Biscardi, E. Iglesia, J. Catal. 222 (2004) 481.
[19] R.D. Cortright, J.A. Dumesic, J. Catal. 148 (1994) 771.
[20] P. Beloen, F.M. Dautzenberg, W.M.H. Sachtler, J. Catal. 50 (1977) 77.
[21] J.K.A. Clarke, Chem. Dev. 75 (1975) 391.
[22] A.C. Muller, P.A. Engelhard, J.E. Weisang, J. Catal. 56 (1979) 65.
[23] J. Beltramini, D.L. Trimm, Appl. Catal. 31 (1987) 113.
[24] S.M. Stagg, C.A. Querini, W.E. Alvarez, D.E. Resasco, J. Catal. 168 (1997) 75.
[25] J.M. Hill, R.D. Cortright, J.A. Dumesic, Appl. Catal. A Gen. 168 (1998) 9.
[26] M. Larsson, M. Hulten, E.A. Blekkan, B. Andersson, J. Catal. 164 (1996) 44.
[27] J. Volter, G. Lietz, M. Uhlemann, M. Hermann, J. Catal. 68 (1981) 42.
[28] M. Santhosh Kumar, De Chen, J.C. Walmsley, A. Holmen, Catal. Commun. 9 (2008) 747.
[29] D. Zhao, J. Feng, Q. Huo, N. Melosh, G.H. Fredrickson, B.F. Chmelka, G.D. Stucky, Science 279 (1998) 548.
[30] M. Santhosh Kumar, J. Perez-Ramirez, M.N. Debbagh, B. Smarsly, U. Bentrup, A. Bruckner, Appl. Catal. B 62 (2006) 244.
[31] G. Jura, W.D. Harkins, J. Chem. Phys. 11 (1943) 430.
[32] J.C. Broekhoff, J.H. de Boer, J. Catal. 10 (1968) 368.

[33] H.P. Rebo, D. Chen, E.A. Blekkan, A. Holmen, Stud. Surf. Sci. Catal. 119 (1998) 617.
[34] B.A. Sexton, A.E. Hughes, K. Forger, J. Catal. 88 (1984) 466.
[35] J.L. Meitzner, G.H. Via, F.W. Lytle, S.C. Fung, J.H. Sinfelt, J. Phys. Chem. 2 (1988) 2925.
[36] R. Burch, J. Catal. 71 (1981) 348.
[37] R.M. Rioux, H. Song, J.D. Hoefelmeyer, P. Yang, G.A. Somerjai, J. Phys. Chem. B 109 (2005) 2192.
[38] M.L. Toebes, Y. Zhang, J. Hájek, T.A. Nijhuis, J.H. Bitter, A.J. van Dillen, D.Y. Murzin, D.C. Koningsberger, K.P. de Jong, J. Catal. 226 (2004) 215.
[39] R.V.V. Hardeveld, F. Hartog, Surf. Sci. 15 (1969) 189.
[40] R.T. Vang, K. Honkala, S. Dahl, E.K. Vestergaard, J. Schnadt, E. Lægsgaard, B.S. Clausen, J.K. Nørskov, F. Besenbacher, Nat. Mater. 4 (2005) 160.
[41] A. Virnovskaia, S. Morandi, E. Rytter, G. Ghiotti, U. Olsbye, J. Phys. Chem. C 111 (2007) 14732.
[42] E. Merlen, P. Beccat, J.C. Bertolini, P. Delichere, N. Zanier, B. Didillon, J. Catal. 159 (1996) 178.
[43] H. Lieske, A. Sarkany, J. Völter, Appl. Catal. 30 (1987) 69.
[44] H. Veerbeck, W.M.H. Sachtler, J. Catal. 42 (1976) 257.
[45] I.B. Yarusov, E.V. Zatolokina, N.V. Shitova, A.S. Belyi, N.M. Ostrovskii, Catal. Today 13 (1992) 655.